Available online at www.sciencedirect.com

jmr&t
Journal of Materials Research and Technology
www.jmrt.com.br

Original Article

A comparative study on the microstructure and mechanical properties of fusion welded 9 Cr-1 Mo steel

S. Madhavan[a,*], M. Kamaraj[b], B. Arivazhagan[c]

[a] Department of Mechanical Engineering, SRM Institute of Science and Technology Kattankulathur, Chennai 603203, India
[b] Department of Metallurgical and Materials Engineering, Indian Institute of Technology Madras, Chennai, 600036, India
[c] Materials Development and Technology Division, Indira Gandhi Centre for Atomic Research, Kalpakkam 603 102, India

ARTICLE INFO

Article history:
Received 27 September 2019
Accepted 17 December 2019
Available online 30 December 2019

Keywords:
P-CMT
P91
Weld
PWHT
Heat input
Toughness

ABSTRACT

Modified 9 Cr–1 Mo is an ideal candidate preferred for high temperature applications in power plants. In this study, three P91 welds of 12 mm thickness are produced using Gas Tungsten Arc Welding (GTAW), Cold Metal Transfer (CMT) and Pulsed-CMT (P-CMT) processes. The impact toughness is evaluated in the as-welded as well as in the PWHT (760 °C-2 h) condition. It is found that P-CMT process resulted in the highest toughness in both the conditions. The heat input was maximum in the case of GTAW (800 J/mm) welds and minimum in CMT (330 J/mm). Even though P-CMT (380 J/mm) has heat input slightly above CMT, the former is compensated by higher welding speeds. Electron microscopy analysis revealed the presence of fine $M_{23}C_6$ and MX precipitates. Among the welds, P-CMT had minimal amount of the precipitates whereas GTAW welds had the maximum. The dimple morphology observed in the ruptured surface significantly varied and P-CMT process had finer dimples indicating finer weld microstructures and enhanced mechanical properties.

1. Introduction

The need to enhance thermal operational efficiency of power plants has been the driving factor for the development of creep-resistant Cr-Mo steels. Though weldability of thick P91 sections has no drawbacks with pre-heating, their creep properties get altered by welding processes and their heat inputs [1,2]. P91 steels are joined using Shielded Metal Arc Welding (SMAW), Gas Metal Arc Welding (GMAW), Submerged arc welding (SAW), GTAW and Activated flux GTAW (A-GTAW) welding. SMAW welding of P91 steel with low hydrogen electrodes resulted in degradation of HAZ toughness compared with the base metal. Metal cored wires are preferred over solid GMAW as the latter results in welding defects like inclusion and lack of fusion [3]. To enhance the deposition rate and to have control over the heat energy supplied Pulsed-GMAW can be employed [4,5]. In contrast with other fusion processes, pulsed process minimizes the heat affected zone and promotes sound joint [6,7]. The A-GTAW process is a mono pass welding categorized by reversed Marangoni flow [8,9] (Marangoni effect refers to flow of fluid caused by a gradient in surface tension. Fluid flows from a region with low surface tension to a region with high surface tension) that results in greater penetrations. Welds produced by processes like electron and laser

* Corresponding author.
E-mail: madhavas@srmist.edu.in (S. Madhavan).
https://doi.org/10.1016/j.jmrt.2019.12.053

beam show elevated creep strengths due to coherent heating. Moreover, electron beam helps in deeper penetrations with narrow fusion zone and minimal distortion but results in type IV cracking due to development of tensile residual stresses. Mechanical properties of laser welded P91 steels processed at different tempering conditions have been investigated. It was reported that reduced heat input and finer welding spot resulted in narrow HAZ. Generally higher cooling rates with minimal heat input will minimize grain coarsening in the HAZ thus preventing type IV cracking in service [10–13].

Regardless of these merits, application remains limited because the process can be put to use only in a high vacuum chamber [2,14,15]. But, development of non-vacuum and local chamber processes in the recent years has opened up a wider window. It is known that higher the heat input, slower is the solidification rate, wider HAZ widths and greater levels of dilutions. Dilution results in solidification cracking and reduction in the toughness of the welds. Dilution here refers to excess movement of constituent elements resulting in degradation of properties. Weld metal toughness is a critical property, which is evaluated during hydrotesting of pressure vessels. Weld should possess a minimum impact energy 45 J. Thermo-mechanical simulator was used to study the PWHT HAZ toughness of P91 welds. It was found that there is fluctuation in the toughness due to changes in the notch position and variation in the path of cracking [16]. Formation of delta ferrite is favoured due to high Cr and Si, which results in cold cracking and degradation of creep properties. To suitably combat this issue, preheat (200–250 °C) and interpass temperature is always maintained. Inter pass helps in diffusing out hydrogen. Presence of delta-ferrite in the fusion zone has been identified as the sole factor responsible for degradation of weld toughness. PWHT at 760 °C for 6 h helps to overcome this degradation [17,18]. Most care should be taken during the PWHT such that the upper limit of heat-treating temperature is less than the actual temperature of transformation on heating to avoid formation of martensite or soft ferrite. Hypothesis claim that preheating at 280 °C before PWHT would be preferable to enhance the impact toughness but fracture morphology changes from fixed to cleavage [19].

Quality weldments with minimal heat inputs are produced using solid state processes. But there are restrictions arising from complex forms and dimensions. Therefore, the need of the hour is to have a melting and joining technique with reduced cost for joining materials with minimum heat input. So, based on the above-mentioned requirements, a new short circuit welding process called the cold metal transfer (CMT) is identified. Compared to the above discussed processes, CMT works on a simple to and fro motion with enhanced welding speeds.

From the above certainties, it is a proven fact that there are limited prior arts available for cold metal transfer (CMT) welding of power plant steels. The primary aim of this work is to establish whether changes in the process and their heat inputs parameters play some role in contributing to the variability in toughness. So, three different processes with High (GTAW), Medium (P-CMT) and Low (CMT) heat inputs are used to produce the welds. Microstructural transitions in these welds are characterized using transmission electron microscopy (TEM). Mechanical properties including hardness, impact toughness are correlated with microstructural features.

2. Experimental procedures

2.1. Materials and welding procedure

Current work makes use of modified 9 Cr-1 Mo steel in the normalized and tempered condition as the base material. The chemical composition of the base metal was analysed and given in Table 1.

2.2. Gas Tungsten Arc welding (GTAW) process

Plates of 12 mm thickness were welded at a heat input of 800 J/mm. Filler rod with a diameter of 2.4 mm was used with pure argon as the shielding gas. Preheating was done at 250 °C and interpass temperature of 200 °C was maintained.

2.3. Cold metal transfer (CMT) and Pulsed-CMT welding process

ER90S-B9 solid metal wire with 1.2 mm diameter was used as the filler metal for preparation of the butt welds. Pre-heat free welding was carried out. Butt Joints were produced using CMT (330 J/mm) and P-CMT (380 J/mm) welding processes. Commercially available $Ar-CO_2$ mixture was purged at a flow rate of 18 lpm (litres per minute) for shielding. The heat input is calculated by using a digitized oscilloscope.

2.4. Radiography

To have an insight about the quality of the weldments and to detect the presence of any significant defects the welds were qualified by x-ray radiography. ^{192}Ir γ-rays was used for the exposure using ASTM NO: 10 penetrameter. The radiograph to be qualified generally shows sensitivity as per 1 T. The exposure time and source to film distance was fixed after several iterations. The weld was qualified with the reference radiograph according to ASME Sec V for gas porosity.

Common metallographic procedures were followed for microstructural analysis. Transverse sections of the weld were cut and polished. Etching was done using Villella's reagent (1 g picric acid +5 ml HCl acid and 100 ml ethanol). Optical and electron microscopy studies were carried out for structure property correlations. Vickers microhardness survey was carried out across the cross weld at a uniform load of 500 gms at regular intervals of 0.1 mm. Charpy V-notch specimens were prepared from the transverse cross-section of the weldments and tested according to ASTM E-23. Scanning electron microscopy (SEM) was used to analyse the fractography of the welds produced by GTAW, CMT and P-CMT processes.

3. Results and discussion

3.1. Radiographic examination of the welds

The radiographic films are exposed by under lighting technique. Fig. 1 shows the radiographic image of the P91 steel

Table 1 – Chemical composition of P91 steel (wt.%).

Materials	C	Cr	Mo	Si	Mn	V	S	P	Ni	Nb
P91	0.12	9.13	0.86	0.27	0.42	0.22	0.02	0.02	0.22	0.06

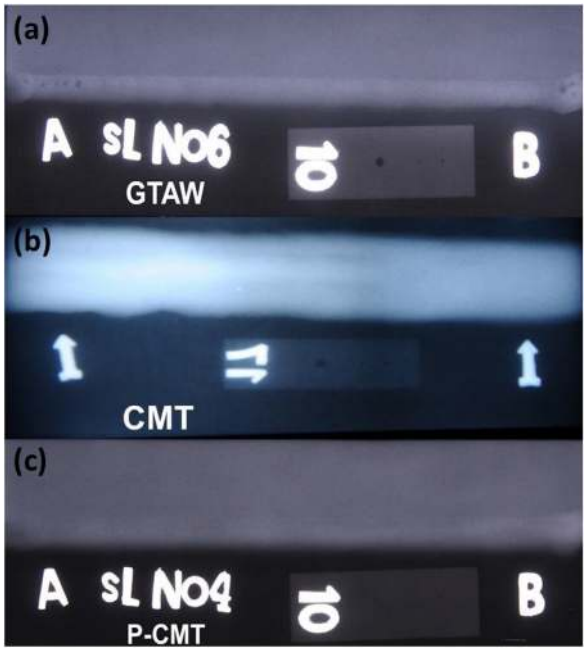

Fig. 1 – X-ray radiograph of P91 steel joint produced by (a) GTAW, (b) CMT and (c) P-CMT processes.

welds produced by GTAW, CMT and P-CMT processes. There are few gas porosities at the beginning and end of the GTAW welds. Whereas, there is no discontinuity in the CMT weld with slight waviness due to the surface appearance. P-CMT weld shown in Fig. 1(c) is free from any defect and the weld zone is perfectly fused without any waviness. This implies that the rate of deposition and the welding parameters are more synchronized than the other processes under investigation.

3.2. *Microstructures*

P91 base metal microstructure consists of uniform grains of ferrite, as the matrix, with tempered martensite [2] Fig. 2. There are also some finer carbides distributed at the grain boundaries of ferrite. These are Nb and V rich (C, N) and $M_{23}C_6$ types [1,2].

A comparison between the welding processes shows that the GTAW welding has more tempered martensite with finer grains Fig. 3(a). It also has minimal volume of δ-ferrite (indicated by arrows, blocky white particles) which is absent in the other low heat input processes. This is because of the stable existence of δ-ferrite in the short range in the L+ δ-ferrite phase field [3]. Generally, in low heat input processes nucleation of δ-ferrite is suppressed and phase transformation takes place from liquid metal to austenite. On the contrary, due to slow rate of cooling, nucleation is also at a reduced pace but aids transformation of ferrite to austenite. δ-ferrite nucleates from the liquid metal at 1524 °C and its stability is limited to 13 °C below. So, at this rate of rapid solidification the formation of δ-ferrite is totally curbed [6]. The weld region of GTAW + PWHT (760 °C-2 h) had a mixture of both tempered and untempered zone, which is probably due to the high heat input and low deposition nature compared to the other processes under study Fig. 3(b).

On the other hand, CMT has fine needles of martensite without any tempering effect and least ferrite phases Fig. 3(c). CMT welding + PWHT altered the microstructure with coarse martensite with acicular ferrite. There are more homogeneous grains of martensite in the ferritic matrix due to the long stress relieving temperature Fig. 3(d).

As -welded fusion zone microstructure of P-CMT joint has dominant martensite, ferrite and dispersion of alloy carbides (V, Nb rich (C, N) and $M_{23}C_6$) as shown in Fig. 3(e). A critical study on these carbides are carried out using TEM and discussed in the subsequent sections. It has less dense martensite leading to reduction in hardness compared to CMT process. The P-CMT + PWHT microstructure has uniformly tempered martensite with uniform ferrite as shown in Fig. 3(f). The cross-sectional macrostructure for all the processes significantly differ due to the variation in heat input and different modes of metal deposition. In the case of GTAW welding the multipass weld bead is clearly visible, whereas CMT and P-CMT welding resulted in complete fusion in spite of the low heat input. This takes place because of the jerky action that occurs instantaneously with short circuiting due to wire retraction, which promotes droplet detachment into the weld pool breaking the dendrites and creating heterogeneous nucleation sites. This effect is more severe due to the pulsating nature of peak currents, which has resulted in maximum toughness in the as-welded and PWHT conditions.

Fig. 4(a, b and c) shows TEM micrographs of weld zone for different processes under consideration at their respective heat inputs. All weld metals contain second phase particles with morphologies varying from process to process indicated by the arrows. The size of precipitates, in particular, being fine in low heat input process and coarse in high heat input process. Fig. 4(a) shows the GTAW welded fusion zone with coagulation of plate like second phase particles with sizes ranging from 175 to 350 nm. The dendritic grain size seems to be coarser compared to CMT and P-CMT processes. With reduction in the heat input (330 J/mm) there is no clustering of the second phase particles; rather they are distributed across the weld zone Fig. 4(b). These particles originate within the ferrite matrix and contribute to its strength. In the case of P-CMT process the particles are ultra-fine (50–75 nm) and pin the boundaries while a few existing on the bulk, Fig. 4(c). Columnar dendrites with uniform spacing without secondary or tertiary arms are also observed. This significant variation in the size and morphology of second phase particles is due to the regular jerky motion of the process. The chances of auto tempering (auto-tempering, a phenomenon in which the first-formed martensite (by quenching) near the martensitic

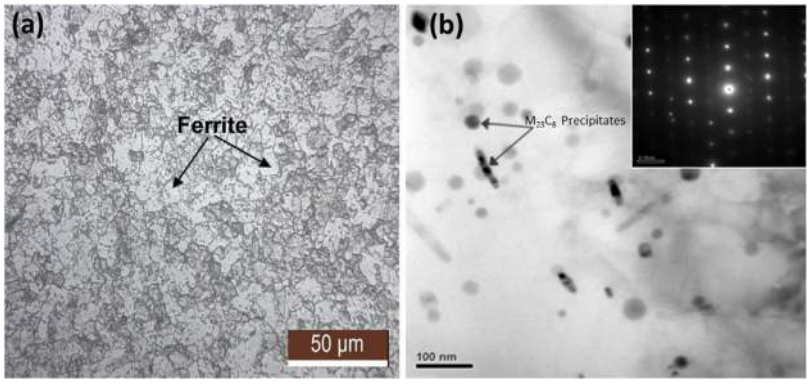

Fig. 2 – (a) Optical micrograph and (b)Transmission electron micrograph of P91 base metal. Inset: SAED pattern of $M_{23}C_6$ precipitates.

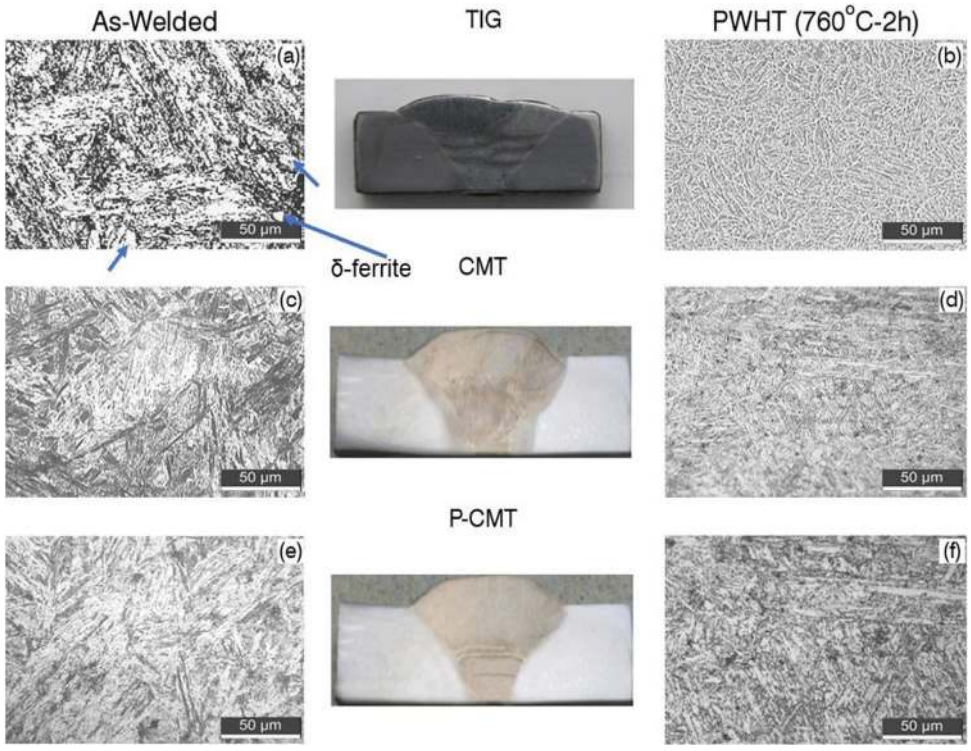

Fig. 3 – Optical micrographs and cross-sectional macrographs of weld zone produced by GTAW, CMT and P-CMT processes in as welded (a, c and e) and PWHT (b, d and f) conditions.

transformation start temperature gets tempered during the remaining process of quenching or cooling. This eliminates the need for a separate tempering after quenching. Such a phenomenon being present or not will be governed by the alloy composition as well as the cooling rate). It is minimal in the case of GTAW welding because of its reduced cooling rates at elevated temperature ranges. On the contrary, welds produced by CMT and P-CMT processes cool rapidly due to reduced heat input compared to GTAW. The auto-tempered martensite that forms because of the welding cooling cycle resulted in the enhancement of the weld toughness [20]. Prior literatures [7,21] reveals that the presence of Ni eliminates carbon, stabilizes austenite and increases the ferrite toughness by absorbing the impact loads and inhibiting the crack initiation. The needle-shaped V, Nb rich (C, N) and $M_{23}C_6$ carbides are observed, Fig. 4(c) in the P-CMT process. The ideal heat input results in the formation of fine grain boundary precipitates which causes an enhanced toughness.

3.3. *Impact toughness and hardness*

The variation of impact toughness in the as-welded and PWHT conditions are shown in Fig. 5. It is found that the welds produced by P-CMT process exhibited the maximum toughness with as-welded: 76 J and PWHT:174 J. Whereas, GTAW welds have the minimum toughness in both the conditions, as-welded: 26 J and PWHT:132 J. The impact energy of CMT and P-CMT welds in the as-welded conditions satisfied the EN: 1557:1997 specification i.e. P91 steel welds require a minimum of 47 J during the hydrotesting of vessels. However, GTAW weld

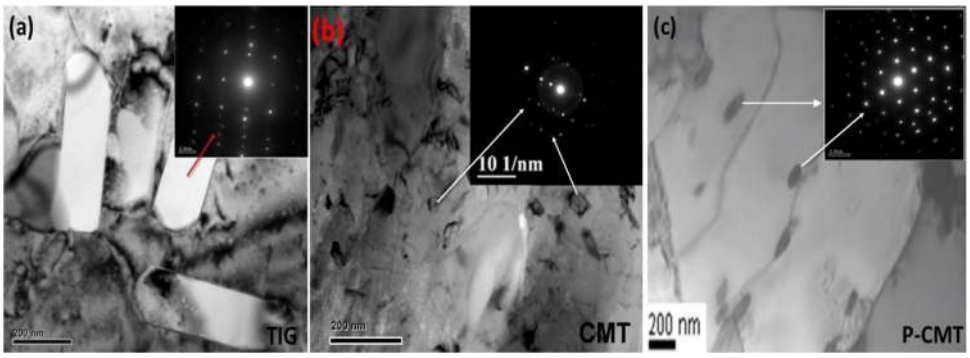

Fig. 4 – TEM micrograph of the weld zone for a) GTAW weld (800 J/mm) with plate like second phase particles, b) CMT weld (330 J/mm) uniformly distributed ultra-fine globular precipitates, c) P-CMT (380 J/mm) with needle like precipitates pinning the dendritic boundaries.

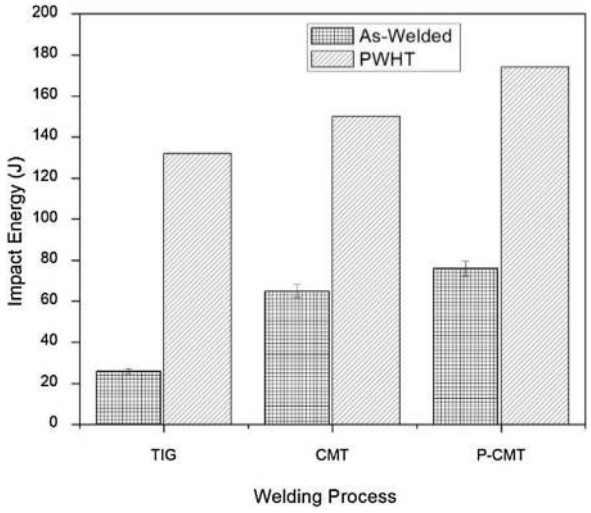

Fig. 5 – Variation of toughness in the as-welded and PWHT conditions for GTAW, CMT and P-CMT processes.

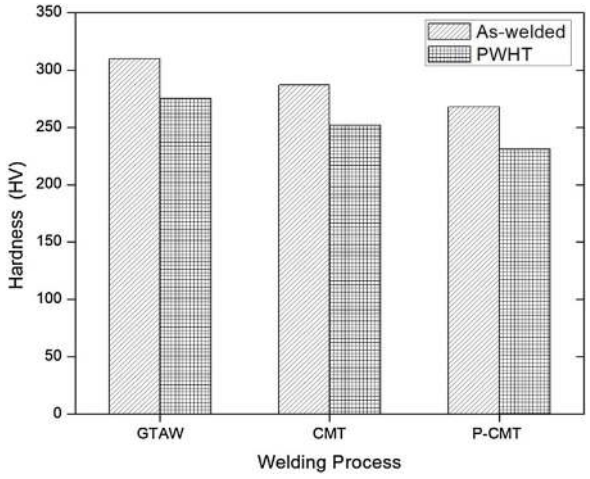

Fig. 6 – Variation of hardness in the as-welded and PWHT conditions for GTAW, CMT and P-CMT processes.

failed to meet in the as-welded condition but satisfied in the PWHT condition. Delta-ferrite, depending on quantity, will transform at lower temperatures to alpha-ferrite and sigma phases. The latter is very brittle. Hence the deleterious effect of increasing delta ferrite content on toughness.

The rise in the magnitude of impact toughness could be due to the finer microstructures obtained with P-CMT process [3]. The variation of hardness in the as-welded and PWHT conditions is shown in Fig. 6. Low heat input welding (CMT and P-CMT) has better toughness with reduced hardness than high heat input (GTAW) process because when the heat input is high more thermal energy is supplied to the weld pool thereby the solidification rates are less. When there are no phase transformations a slower solidification leads to uniform contractions from the exterior surface to the interior, which results in coarse dendrites.

In the case of CMT process the heat extraction is along the direction of welding. As a result, surface cools faster due to convective heat transfer and the material present in the interior starts to cool instantaneously, layer by layer, which results in finer grains with enhanced toughness. With rise in heat input the δ-ferrite content in weld increases thereby, decreasing the toughness. In GTAW welds, δ-ferrite might not be the only factor for reduction in toughness it is also governed by the precipitate morphology, thermodynamics and kinetics associated with the solidification [22]. In the as-welded condition, hardness is high due to untempered martensite. In GTA weld, due to multipass and inter-bead tempering effects hardness is less. In the case of CMT and P-CMT, due to enhanced cooling fine martensite was observed than GTAW weld. After PWHT, due to tempering, martensite losses its tetragonality and reaches its stable state. Since, PWHT reduces the dislocation density and solid solution strengthening. All the above-mentioned effects cause reduction in hardness after PWHT.

3.4. *Fractographic morphology studies*

Fracture micrographs of the welds produced using different processes are shown in Fig. 7. In the as-welded condition, irrespective of the process, there are no dimples on the fracture surface but flat facets with tiny step-like appearance are present in Fig. 7(a), (c) and (e). On the contrary, PWHT weld

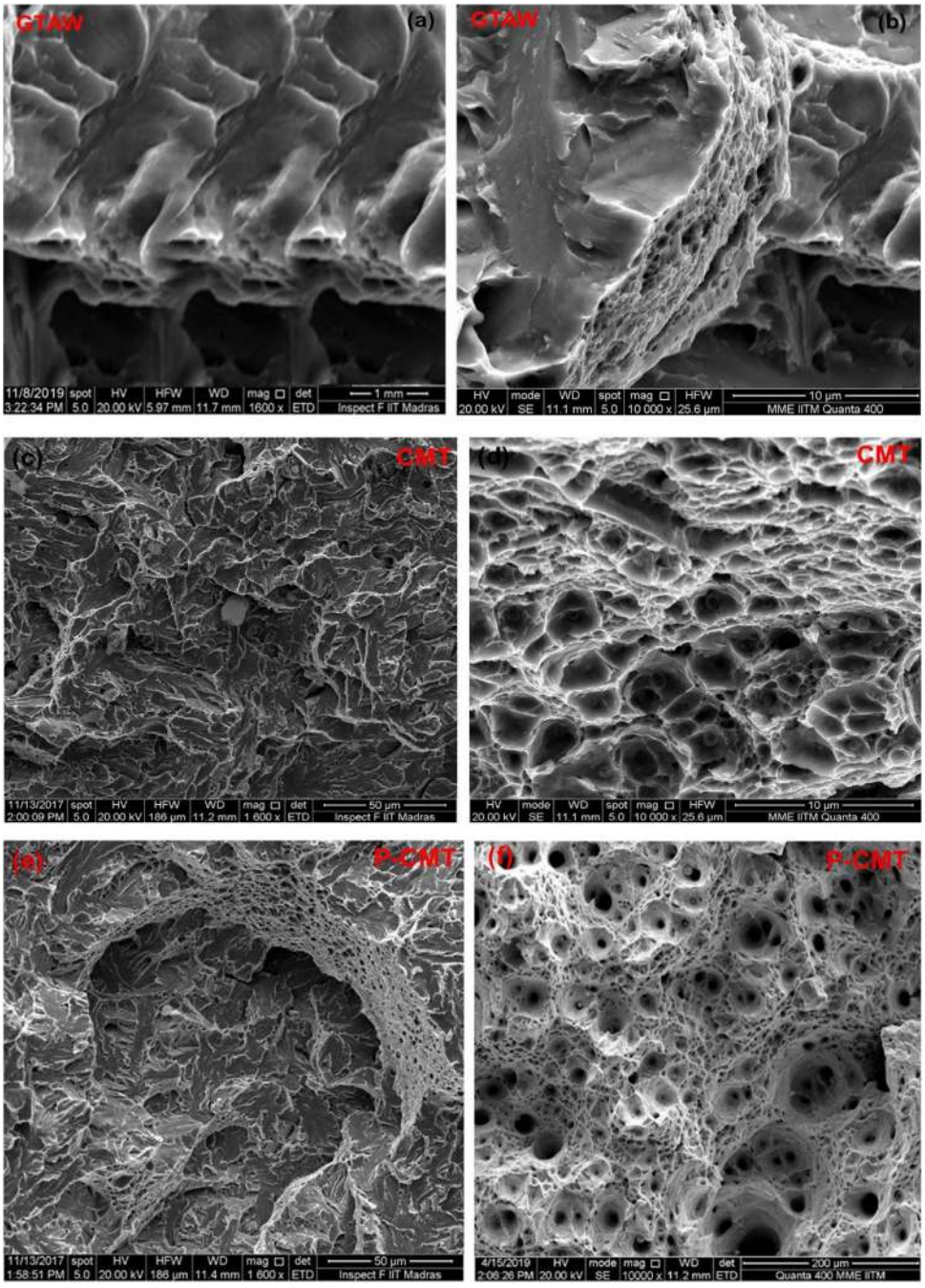

Fig. 7 – Scanning electron micrographs (secondary electron mode-Everhart Thornley detector) of the weld fracture produced by GTAW, CMT and P-CMT processes in the as welded (a, c and e) and PWHT (b, d and f) conditions.

fracture surfaces have dimples of varying sizes. Precipitates or second phase particles are commonly believed to be responsible for the initiation of micro voids [23].

Even when they are present in a relatively small quantity these particles often play a direct role in initiation of dimples. The dimple size is found to be the least for P-CMT process Fig. 7 (f) and highest for GTAW Fig. 7(b). Finer dimples usually contribute to improved toughness of the weldments. Electron microscopy analysis reveals presence of wide cavities, Fig. 7(d), with their axes along the direction of shearing. The dimples produced by tensile shearing are in the opposite directions of the fracture surfaces.

4. Summary and conclusions

Butt welds of Modified 9 Cr–1 Mo steel were successfully produced by GTAW, CMT and P-CMT processes. The effect of process-associated heat inputs on the microstructure and impact toughness of the joints are analysed. From this investigation, the following conclusions are derived.

i Pulsed-cold metal transfer process resulted in high impact toughness and hardness. The impact toughness is evaluated in the as-welded as well as in the PWHT (760 °C-2 h) condition. The impact energy of CMT and P-CMT welds in the as-welded conditions satisfied the EN: 1557:1997 specification. It is found that P-CMT process resulted in the highest toughness in both the conditions.

ii Weld zone of P-CMT had minimal amount of the finer precipitates present at the boundaries whereas GTAW welds had coarse second phase particles.

iii In GTAW welds, δ-ferrite is not the sole factor for degradation of toughness. It is also controlled by the kinetics associated with the process. Low heat input welding (CMT and P-CMT) had negligible δ-ferrite in the weld zone.

iv As-welded fractography, irrespective of the process, have flat facets with step-like appearance. On the contrary, PWHT weld fracture surfaces have dimples of varying sizes. The dimple size is found to be the least for P-CMT process and the highest for GTAW. Finer dimples usually contribute to improved toughness of the weldments.

Uncited references

[24,25,26].

Appendix A. Supplementary data

Supplementary material related to this article can be found, in the online version, at doi:https://doi.org/10.1016/j.jmrt.2019.12.053.

REFERENCES

[1] Onizawa T, Wakai T, Ando M, Aoto K. Effect of V and Nb contents on mechanical properties of high Cr steel. Proc ECCC Creep Conf 2005:130–42.

[2] Jones WB, Hills CR, Polonis DH. Microstructural evolution of modified 9Cr–1Mo steel. Metall Trans A 22A 1991;5:1049–58.

[3] Shanmugarajan B, Padmanabham G, Kumar H, Albert SK, Bhaduri AK. Autogenous laser welding investigations on modified 9Cr–1Mo (P91) steel. Sci Technol Weld Join 2011;16(6):528–34.

[4] Zhang S, Melfi T, Narayanan BK. Effects of precipitates on mechanical properties of P91 submerged arc welds. Sci Technol Weld Join 2016;21(2):147–56.

[5] Abe F, Tabuchi M, Tsukamoto S, Shirane T. Microstructure evolution in HAZ and suppression of Type IV fracture in advanced ferritic power plant steels. Int J Press Vessel Pip 2010;87:598–604.

[6] Hald J. Metallurgy and creep properties of new 9-12%Cr steels. Steel Res 2009;67:369–74.

[7] Abd El-Azim ME, El-Desoky OE, Ruoff H, Kauffmann F, Roos E. Creep fracture mechanism in welded joints of P91 steel. Mater Sci Technol 2013;29(9):1027–33.

[8] Heiple CR, Roper JR. Effect of Selenium on GTAW fusion zone geometry. Weld J 1981;60:143–5.

[9] Velarde Manuel G. On the importance of nucleation solutions for the rupture of thin liquid films. Philos Trans A Math Phys Eng Sci 1998;356:829–44.

[10] Kiyohide T, Hiroyoshi N. Weld metal impact toughness of electron beam welded 9% Ni steel. Met Construction Nov 1978:536.

[11] Ellis FV, Henry JF, Roberts BW. Influence of Service Exposure on Base and Weld Metal of 1/2 Cr-1/2 Mo-1/4 V High-Pressure Steam Inlet Piping. Pressure Vessels and Piping of ASME 1990;201:55–63.

[12] Okabayashi H, Kume R. Effects of Pre- and Post-Heating on Weld Cracking of 9Cr-1Mo-Nb-V Steel. Trans Jpn Weld Soc 1988;19:63–8.

[13] Onoro J. Martensite Microstructure of 9-12%Cr Steels Weld Metals. J Mater Process Technol 2006;180:137–42.

[14] Francis JA, Mazur W, Bhadeshia HKDH. Type IV cracking in ferritic power plant steels. Mater Sci Technol 2006;22:1387–95.

[15] Chen Liang, Yamashita Ken. Effects of PWHT Temperature on Mechanical Properties of High-Cr Ferritic Heat-Resistant Steel Weld Metals. Weld World 2012;56:81–91.

[16] Silwal B, Li L, Deceuster A, Griffiths B. Effect of postweld heat treatment on the toughness of heat-affected zone for Grade 91 steel. Weld J 2013;92:80–7.

[17] Krishnan S, Kulkarni DV, De A. Probing pulsed current gas metal arc welding for modified 9Cr–1Mo steel. J Mater Eng Perform 2014;24:1411.

[18] Ghosh PK, Devakumaran K, Randhawa HS. Characteristics of a pulsedcurrent, vertical up gas metal arc weld in steel. Metall Mater Trans A 2000;31A:2247–59.

[19] Pandey C, Mahapatra MM. Evolution of phases during tempering of P91 steel at 760°C for varying tempering time and their effect on microstructure and mechanical properties. J Mater Eng Perform 2016;25:2195–210.

[20] Sangho Kim SL, Young-RocIm, Lee Hu-Chul, Yong Jun Oh, Hwa Hong JUN. Effects of alloying elements on mechanical and fracture properties of base metals and simulated heat-affected zones of SA 508 steels. Metall Mater Trans A 2001;32:903–11.

[21] Tavares SSM, Pardal JM, Souza GC, Garcia PSP, Barbosa ES, Barbosa C, et al. Study of cracks in the weld metal joint of p91 steel of a superheater steam pipe. Eng Fail Anal 2015;56:464–73.

[22] Arivazhagan B, Vasudevan M. A comparative study on the effect of GTAW processes on the microstructure and mechanical properties of P91 steel weld joints. J Manuf Process 2014;16:305–11.

[23] Noell Philip, Carroll Jay, Hattar Khalid, Clark Blythe, Boyce Brad. Do voids nucleate at grain boundaries during ductile rupture? Acta Mater 2017;137:103–14.

[24] Kondo M, Tabuchi M, Tsukamoto S, et al. Suppressing type IV failure via modification of heat affected zone microstructures using high boron content in 9Cr heat resistant steel welded joints. Sci Technol Weld Joining 2006;11:216–23.

[25] Devakumaran K, Ghosh PK. Thermal Characteristics of Weld and HAZ during Pulse Current Gas Metal Arc Weld Bead Depositinion of HSLASteel Plate. Mater Manuf Processes 2010;25:616–30.

[26] Kamal P, Surya KP. Effect of Pulse Parameters on Weld Quality in Pulsed Gas Metal Arc Welding: A Review. J Mater Eng Perform 2011;20:918–31.